FISEVIER

Contents lists available at ScienceDirect

Science of the Total Environment

journal homepage: www.elsevier.com/locate/scitotenv



Natural organic matter inhibits Ni stabilization during Fe(II)-catalyzed ferrihydrite transformation



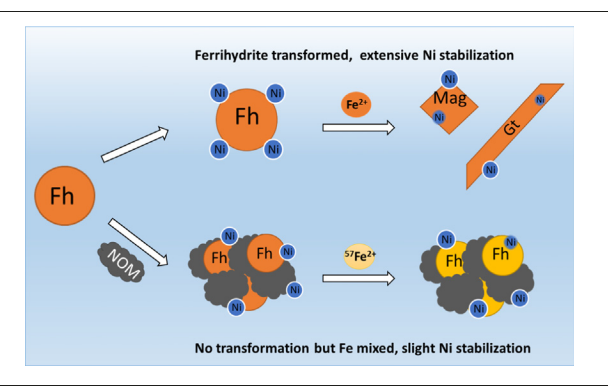
Zhe Zhou ^{a,b,*}, Drew E. Latta ^a, Michelle M. Scherer ^a

- ^a Department of Civil & Environmental Engineering, The University of Iowa, Iowa City, United States
- ^b Alfred Wegener Institute Helmholtz Centre for Polar and Marine Research, Bremerhaven, Germany

HIGHLIGHTS

- Ni is released and re-sorbed during Fe (II)-catalyzed ferrihydrite (Fh) transformation
- Ni stability increases when Fh transforms into secondary Fe minerals.
- Natural organic matter (NOM) inhibits Fh transformation and Ni stabilization.
- Only Fe atom exchange between Fe(II) and Fh cannot obviously increase Ni stability.

GRAPHICAL ABSTRACT



ARTICLE INFO

Article history: Received 17 July 2020 Received in revised form 23 September 2020 Accepted 23 September 2020 Available online 30 September 2020

Editor: Xinbin Feng

Keywords: Natural organic matter Ferrihydrite Nickel Mineral transformation Fe atom exchange

ABSTRACT

Trace metals, such as nickel (Ni), are often found associated with ferrihydrite (Fh) in soil and sediment and have been shown to redistribute during Fe(II)-catalyzed transformation of Fh. Fe(II)-catalyzed transformation of Fh, however, is often inhibited when natural organic matter (NOM) is associated with Fh. To explore whether NOM affects the behavior of Ni during Fe(II)-catalyzed transformation of Fh, we tracked Ni distribution, Fe atom exchange, and mineral transformation of Fh and Fh coprecipitated with Suwannee River natural organic matter (SRNOM-Fh). As expected, in the absence of Fe(II), Fh and SRNOM-Fh did not transform to secondary Fe minerals after two weeks. We further observed little difference in Ni adsorption on SRNOM-Fh compared to Fh. In the presence of Fe(II), however, we found that Ni associated with SRNOM-Fh was more susceptible to acid extraction than Fh. Specifically, we found almost double the amount of Ni remaining in the Fh after mild extraction compared to SRNOM-Fh. XRD showed that Fh transformed to goethite and magnetite whereas SRNOM-Fh did not transform despite ⁵⁷Fe isotope tracer experiments confirmed that SRNOM-Fh underwent extensive atom exchange with aqueous Fe(II). Our findings suggest that Fe atom exchange may not be sufficient for obvious Ni stabilization and that transformation to secondary minerals may be necessary for Ni stabilization to occur.

© 2020 Elsevier B.V. All rights reserved.

1. Introduction

Ferrihydrite (Fh), a short-range ordered Fe mineral, is widely distributed in soils and sediments (Cornell and Schwertmann, 2003;

E-mail address: zhe_research@outlook.com (Z. Zhou).

Schwertmann and Fischer, 1973). Considering its nanoscale size and abundant surface functional groups, Fh is also regarded as an important natural sorbent for natural organic matter (NOM) and trace metals (such as Ni) (Cornell and Schwertmann, 2003; Lalonde et al., 2012). Fh and aqueous Fe(II) often coexist at redox interfaces in soils and sediments (Melton et al., 2014; Weber et al., 2006). Redox reactions between Fe(II) and Fe(III) in Fh result in the formation of secondary Fe minerals (Hansel et al., 2005; Pedersen et al., 2005), and is linked to

^{*} Corresponding at: Alfred Wegener Institute Helmholtz Centre for Polar and Marine Research. Bremerhaven. Germany

cycling of other important elements, such as C, N, P and trace metals (Gorski and Scherer, 2011; Voelker et al., 1997; Li et al., 2012; Van Cappellen and Wang, 1996).

Fe(II)-catalyzed Fh transformation to secondary minerals (Hansel et al., 2003; Tronc et al., 1992) has been found to redistribute trace metals that associated with Fh through adsorption and coprecipitation (Martinez and McBride, 1998; Vu et al., 2013; Liu et al., 2016; Latta et al., 2012a). Specifically, structural incorporation of metals into secondary Fe minerals during Fh transformation has been suggested for Cu²⁺, Zn²⁺, Mn²⁺, Co²⁺, Sb⁵⁺, As⁵⁺ and U⁶⁺ (Liu et al., 2016; Latta et al., 2012a; Mitsunobu et al., 2013; Bolanz et al., 2013; Muramatsu et al., 2012; Marshall et al., 2014; Jang et al., 2003). Spectroscopic evidence of this structural incorporation has been shown for As⁵⁺ and Sb⁵⁺ (Mitsunobu et al., 2013; Bolanz et al., 2013; Muramatsu et al., 2012). Metals structurally incorporated into secondary Fe minerals were found to be more stable (Fei et al., 2018; Liu et al., 2016) and the incorporated trace metal may also alter the properties of the secondary Fe minerals (Vu et al., 2013; Liu et al., 2016).

Similar to trace metals, natural organic matter (NOM), resulting from the decomposition of plant and animal matter, is frequently found associated with Fe minerals in soil and sediments (Lalonde et al., 2012; Kaiser and Guggenberger, 2000; von Lutzow et al., 2006). NOM has been shown to alter Fe(II)-catalyzed Fh transformation pathways (Schwertmann, 1966; Chen et al., 2015). For example, with an increasing C/Fe ratio, more Fh was preserved in the presence of Fe(II) until the Fh transformation was inhibited. NOM effectively stabilized Fh from the secondary mineral transformation in the presence of Fe(II). However, NOM was also observed to act as an electron shuttle during the bio-reduction of Fh (Kappler et al., 2004; Shimizu et al., 2013), indicating the electron transfer between Fe(II) and Fh may not be necessarily inhibited by NOM. Our previous work provided direct evidence for both electron transfer and Fe atom exchange between Fe(II) and Fe minerals in the presence of different species of NOM, including humic acid, fulvic acid, and NOM collected by reverse osmosis membrane (Latta et al., 2012b; Zhou et al., 2018). It remains, however, unclear whether Fe atom exchange in the absence of Fh transformation affects the stability of trace metals associated with Fh, such as Ni.

For other minerals, such as goethite and hematite, Ni incorporation or release has been observed during Fe(II)-catalyzed recrystallization without the formation of any secondary Fe minerals (Coughlin and Stone, 1995; Frierdich et al., 2011). Fe atom exchange between aqueous Fe(II) and Fe(III) minerals were suggested to facilitate Ni re-distribution (Frierdich et al., 2012). It is unknown, however, whether Ni stabilization occurs during the reaction between aqueous Fe(II) and Fh with coprecipitated NOM as we have shown extensive Fe atom exchange occurred (Zhou et al., 2018; Chanda et al., 2020). Here, we investigated the effect of coprecipitated Suwannee River NOM (SRNOM) on Ni stabilization during Fe(II)-catalyzed Fh transformation. Specifically, we investigated (i) the fate of adsorbed Ni in Fh and Fh coprecipitated with SRNOM during the reaction with Fe(II) and (ii) the release of preincorporated Ni in Ni-Fh coprecipitate and Ni-SRNOM-Fh coprecipitate in the presence of Fe(II). Our findings provide new insights into the fate of Ni in complex systems that approximate natural environments.

2. Materials and methods

2.1. Synthesis and characterization of Fh minerals

Four different Fe solids were synthesized and used in this study, including pure 2-line Fh, Fh coprecipitated with SRNOM (SRNOM-Fh), Fh coprecipitated with SRNOM and Ni (Ni-SRNOM-Fh). 2-line Fh was synthesized following the method described by Schwertmann, et al. (Schwertmann and Cornell, 2008) The method was modified to synthesize the coprecipitate of SRNOM-Fh by dissolving SRNOM and ferric nitrate (C/Fe ratio 1.6) together before the adding of 1 M KOH, same as we described before (Zhou et al.,

2018). SRNOM was purchased from the International Humic Substance Society and used without further processing. Ni-Fh was synthesized by slowly adding 1 M KOH into a 200 mL solution containing 25 mM ferric nitrate and 1.5 mM Ni(II) chloride (Ni/Fe ratio 0.06) until pH 7.5 was reached in the solution. Vigorous stirring was applied during the whole process. A similar synthesis method was used to prepare Ni-SRNOM-Fh coprecipitate but with an extra 188 mg SRNOM dissolved (C/Fe ratio 1.6) prior to the adding of 1 M KOH. All the solids were washed with deionized water for 3 times and stored as wet in an anaerobic glovebox (7% H₂ and 93% N₂). The synthesized solids were characterized with X-ray diffraction (XRD, Rigaku Mini Flex II) and 57 Fe Mössbauer spectrometer (Web Research Inc., Edina, MN) and used within 7 days. More information about the characterization of the synthesized solid can be found in the supporting information.

2.2. Ni adsorption experiments

The adsorption of aqueous Ni by Fh and SRNOM-Fh was conducted in the anaerobic glovebox. Triplicate bottles were set for all experiments. Each bottle consisted of 1 mM Ni(II), 10 mM PIPES buffer, and 10 mM NaCl (for ionic strength). ⁵⁷Fe labeled aqueous Fe(II) (~97% of ⁵⁷Fe) was added to obtain 1 mM Fe(II) in certain setups. Fh and SRNOM-Fh were then added to get 10 mM Fe(III) in each reactor. The pH was adjusted back to pH 7.0 \pm 0.05 using 1 M KOH. The reactors were rotated on end-over-end rotators while wrapped in aluminum foil. 1 mL aliquots at each time point were sampled and centrifuged. The supernatant was filtered through 0.22 µm filters to get aqueous samples. Centrifuged solids were resuspended in 1 mL 10 mM Piperazine-N, N'- bis (3-propanesulfonic Acid, PIPPS) solution at pH 3.0 for 20 min as a mild Ni extraction. The extraction solution was centrifuged again to get the supernatant as the extracted sample. No structural Fe(III) was dissolved during this extraction. After mild extraction, the residual solids were dissolved by adding 1 mL 5 M HCl to measure the residual Ni. Fe(II) and Ni concentration in aqueous samples, extracted samples, and the samples with dissolved residual solids were measured separately with 1,10-Phenanthroline method and ICP-MS (Zhou et al., 2018). Fe isotope composition in each sample was also analyzed as the method described below. One reaction bottle was sacrificed at each time point and the whole bottle of solution was filtered through an 0.44 µm paper filter to prepare XRD samples.

2.3. Ni release experiments

The distribution of Ni in Ni-Fh and Ni-SRNOM-Fh coprecipitate with or without reaction with Fe(II) was probed by macroscopic Ni release, mild extraction, and acid dissolution. Triplicate reactors were set for each experiment. The coprecipitates were set in 10 mM PIPES buffer at pH 7.0 with or without 1 mM Fe(II) labeled with ⁵⁷Fe. Different solids were first collected by centrifugation and resuspended in 10 mL of 0.1 M HCl. 1 mL aliquots reacted over 2 min, 5 min, 15 min, 30 min, 60 min, and overnight were collected and the concentration of dissolved Ni and total Fe were measured as described above. Samples were analyzed as described in the Ni adsorption experiments to measure aqueous Ni (II), extracted Ni(II), and residual Ni(II). Ni-SRNOM-Fh coprecipitates before and after reaction with Fe(II) were also leached with 0.1 M HCl.

2.4. Fe isotope measurement

For 57 Fe labeled Fe(II) experiments, the Fe isotope composition in aqueous Fe, extractable Fe, and residual solid Fe was analyzed with a quadrupole ICP-MS. The He gas mode with a collision cell was applied to remove isobaric interferences with normal Argon (predominantly 40 Ar 16 O and 40 Ar 16 O 1 H) for 56 Fe and 57 Fe. All samples were diluted with 0.1 M trace metal grade HCl to get Fe concentration under 30 μ M. An internal standard of 3 μ M 59 Co was added to monitor the stability of ICP-MS between different samples. Fe standard solution (natural

abundant) purchased from Agilent and the same batch of enriched ⁵⁷Fe (II) stock solution were used for monitoring the reproducibility and precision of the instrument among different measurements. ⁵⁷Fe percentage was calculated with the count of ⁵⁷Fe divided by the sum count of ⁵⁴Fe, ⁵⁶Fe, ⁵⁷Fe, and ⁵⁸Fe. Triplicate measurements were conducted for each sample.

3. Results and discussion

3.1. Effect of NOM on Ni adsorbed by Fh

To explore whether NOM affects the fate of Ni adsorbed by Fh, we first tracked Ni sorption by Fh and SRNOM-Fh in the absence and presence of Fe(II). In the absence of Fe(II), the extent and rate of Ni sorption by Fh and SRNOM-Fh were similar, with around 60% of Ni removed from aqueous within two hours and almost 80% within one day (Fig. 1a). This first rapid sorption step was followed by a much slower step with an additional 5% sorption over almost two weeks. Two sorption steps are consistent with other studies conducted under similar pH where the formation of the inner-sphere sorption complex was invoked to explain the fast sorption and surface diffusion was invoked to explain the second, slower sorption (Society, n.d.; Scheinost et al., 2001).

To further explore how Ni was associated with the Fh and SRNOM-Fh, we extracted the solids at pH 3.0. No Fe(III) was dissolved in the pH 3.0 extraction. A similar amount of Ni ($430\pm20\,\mu\text{M}$) was extracted from Fh throughout the experiment but the residual Ni increased steadily as the aqueous Ni decreased. The increased amount of Ni in the residual Fh is consistent with the surface diffusion occurring during the second slower Ni adsorption in Fh and SRNOM-Fh, as Ni's diffusion

into the inner structure of Fh makes it less susceptible to weak acid extraction (Bruemmer et al., 1988).

Ni sorption to Fh and SRNOM-Fh in the presence of Fe(II) was also investigated. The aqueous Ni(II) concentration in the presence of Fh and Fe(II) decreased to 107 \pm 8 μM over two weeks, which was lower than 149 \pm 1 μM observed in the absence of Fe(II) (Table S1). Instead of competing with Ni for sorption sites, it appears that Fe(II) slightly enhanced the rate and extent of Ni sorption by Fh (Fig. 1c). In contrast, Ni sorption onto SRNOM-Fh was inhibited by aqueous Fe (II) with 161 \pm 12 μM Ni remaining in the aqueous phase compared to 119 \pm 8 μM in the absence of Fe(II). Based on the aqueous Ni data alone, it appears that Fe(II) slightly enhanced Ni sorption by Fh and slightly inhibited Ni sorption by SRNOM-Fh coprecipitate.

To characterize the Ni further, we acid-extracted Ni and measured the residual Ni by completely dissolving the solids. We found that the presence of Fe(II) extensively decreased the amount of Ni extracted from Fh and increased the amount of residual Ni remaining in the solids (Fig. 1a&c). Ni recovery from the aqueous, extracted, and residual phases was near-complete (91 \pm 5%). We used the percent of Ni extracted from solid-bound Ni (extracted + residual) as an indicator for Ni stability in the solid phase. The extractable Ni in Fh equilibrated without Fe(II) is about 51%. Whereas in the presence of Fe(II), the extractable Ni decreased substantially to 17% suggesting that Ni was more stable in the Fh solids after reaction with Fe(II). In contrast, Fe(II) had little effect on Ni stability in SRNOM-Fh with the extractable Ni decreasing only from 52% to 47% when Fe(II) was added. Previous work showed NOM influenced products formed from Fe(II)-catalyzed transformation of Fh which we suspect is the likely explanation for the different Ni stability within Fh and SNROM-Fh in the presence of Fe(II) (Chen et al., 2015; Zhou et al., 2018).

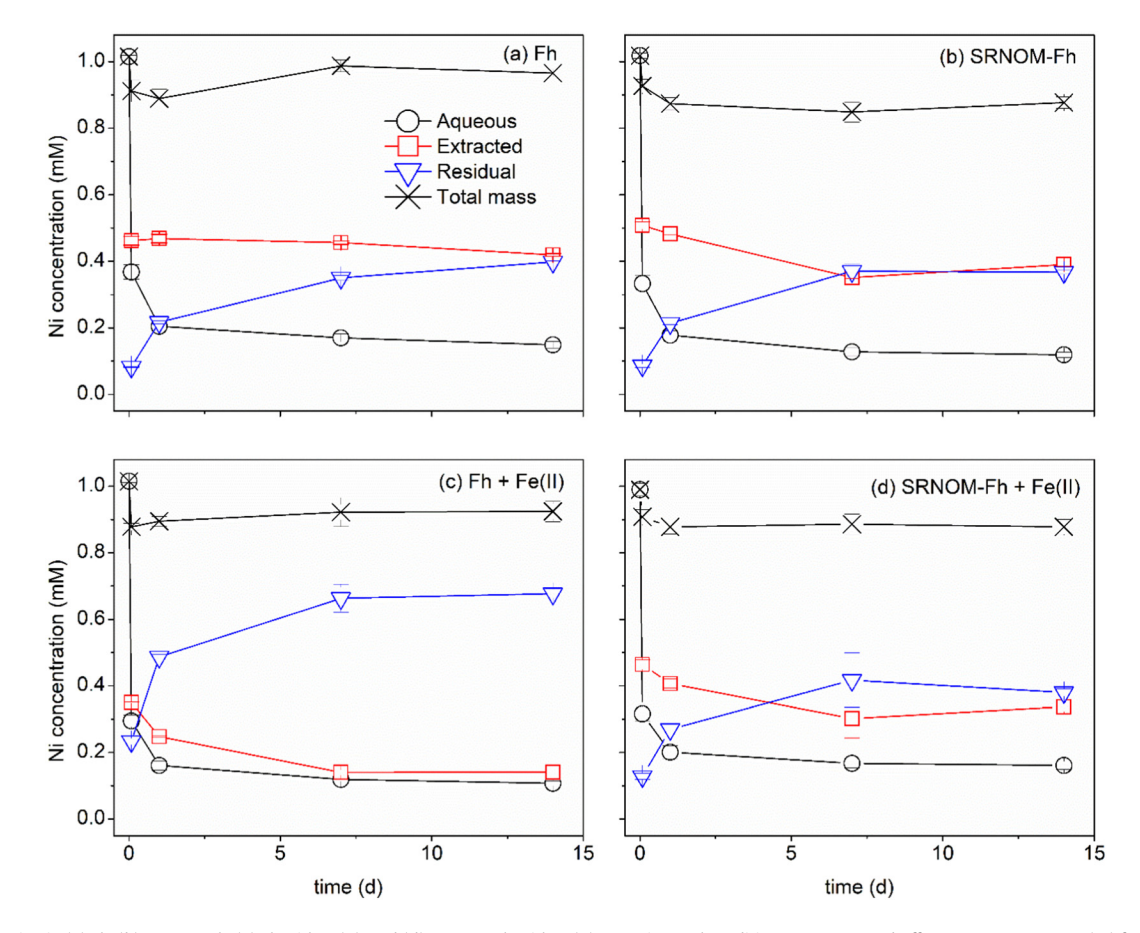


Fig. 1. Ni distribution in (a) Fh, (b) SRNOM-Fh, (c) Fh with Fe(II), and (d) SRNOM-Fh with Fe(II). Experimental condition: 10 mM PIPES buffer at pH 7.0, 10 mM Fe(III) from Fh or SRNOM-Fh, 1 mM Fe(II) in figure (c) and (d). The data points represent the average value and standard deviation in triplicate bottles. More information can be found in Table S1–2.

To test this hypothesis, we tracked the Fe mineralogy change in Fh and SRNOM-Fh after Ni sorption with or without Fe(II) using XRD (Fig. 2). No clear identical diffraction was observed for Fh and SRNOM-Fh without Fe(II), indicating that Fh is not transformed into secondary minerals. Reacting Fh with 1 mM Fe(II) and 1 mM Ni(II) resulted in the formation of goethite and magnetite as shown in the XRD patterns. Fe(II)-catalyzed transformation of Fh into magnetite and goethite has been widely reported (Hansel et al., 2005; Pedersen et al., 2005), and it appears that the presence of Ni under our conditions does not alter the transformation pathway. In contrast to Fh, aqueous Fe (II) did not transform SRNOM-Fh into sufficient secondary Fe minerals to be observed in XRD (Fig. 2). Inhibited Fh transformation with coprecipitated NOM at high C/Fe ratio is consistent with what we and others reported, and the inhibited Ostwald ripening and oriented aggregation of Fh were suggested as possible inhibition mechanisms (Chen et al., 2015; Zhou et al., 2018; ThomasArrigo et al., 2019). Note, however, that Fe atom exchange between aqueous Fe(II) and structural Fe(III) may still occur in the lack of ferrihydrite transformation suggesting that SRNOM-Fh still dynamically mixed with aqueous Fe(II) (Zhou et al., 2018).

To further investigate Fe atom movement between aqueous Fe(II) and SRNOM-Fh with adsorbed Ni(II), we used ⁵⁷Fe(II) and measured Fe(II) mass and isotope composition changes over time. Around 50% of Fe(II) was adsorbed by SRNOM-Fh over 1 h and the percentage of ⁵⁷Fe in aqueous Fe(II) dropped from 97% to 25% accompanied by a rapid increase in solid Fe (from 2.3% to 10%, Table S5). The initial rapid Fe isotope mixing was followed by a further mixing over fourteen days, and the Fe isotope composition in the aqueous and solid Fe phase eventually approached complete isotopic mixing value (Fig. 3a). Since it was unclear if the Fe isotopes were homogeneously distributed in the solid phase, we chose not to quantify the percent of atom exchange based on the homogenous model but rather concluded that extensive Fe atom exchange occurred between aqueous Fe(II) and solid Fe in the presence of both SRNOM and adsorbed Ni (Zhou et al., 2018; Gorski and Fantle, 2017; Joshi et al., 2017). The Fe atom exchange,

however, did not appear to influence Ni stability as a similar amount of residual Ni was measured in SRNOM-Fh with or without Fe(II) (Fig. 1b&d, Table S2).

3.2. Effect of NOM on Ni coprecipitated with Fh

Ni can associate with Fh not only through adsorption but also coprecipitation. To investigate the effect of NOM on the stability of coprecipitated Ni in Fh, we synthesized Ni-Fh and Ni-SRNOM-Fh coprecipitate, and tracked Ni and Fe mineralogical change under reducing condition simulated with aqueous Fe(II). In the absence of Fe(II), there was about 2% of pre-coprecipitated Ni released from Ni-Fh and Ni-SRNOM-Fh into the aqueous phase, possibly due to the reequilibration in a new aqueous system (Fig. 4). The presence of 1 mM Fe(II) increased the concentration of aqueous Ni in the first two hours, about 14% of the coprecipitated Ni was released from Ni-Fh. But the concentration of aqueous Ni dropped over longer reaction time, indicates that the released Ni within the first two hours was resorbed by the solid over time. After fourteen days, the presence of Fe(II) resulted in even lower aqueous Ni concentration in the Ni-Fh experiment (Table S3). Similar to Ni-Fh, Fe(II) also increased Ni release from Ni-SRNOM-Fh in the early stage, but the resorption process was much slower than Ni-Fh. After fourteen days, aqueous Ni concentration increased by about 20 µM in the presence of Fe(II) (Table S4). The Ni released from Ni-SRNOM-Fh coprecipitate in the presence of Fe(II) accounted for $7 \pm 1\%$ of the overall Ni pre-incorporated in the solids (Fig. 4b). Similar amounts of Ni release have been observed for goethite where ~8% of pre-incorporated Ni was released by reacting with Fe(II) (Frierdich and Catalano, 2012).

To investigate the Ni stability in the solid phase, the mild extraction at pH 3.0 was also applied to the experiments with Ni-Fh and Ni-SRNOM-Fh. We found aqueous Fe(II) increased the stability of Ni in Ni-Fh, as the fraction of extractable Ni decreased to 4.7% compared to 35.2% in the absence of Fe(II) (Table S3). Whereas in Ni-SRNOM-Fh, other than an increased aqueous Ni concentration caused by Fe(II),

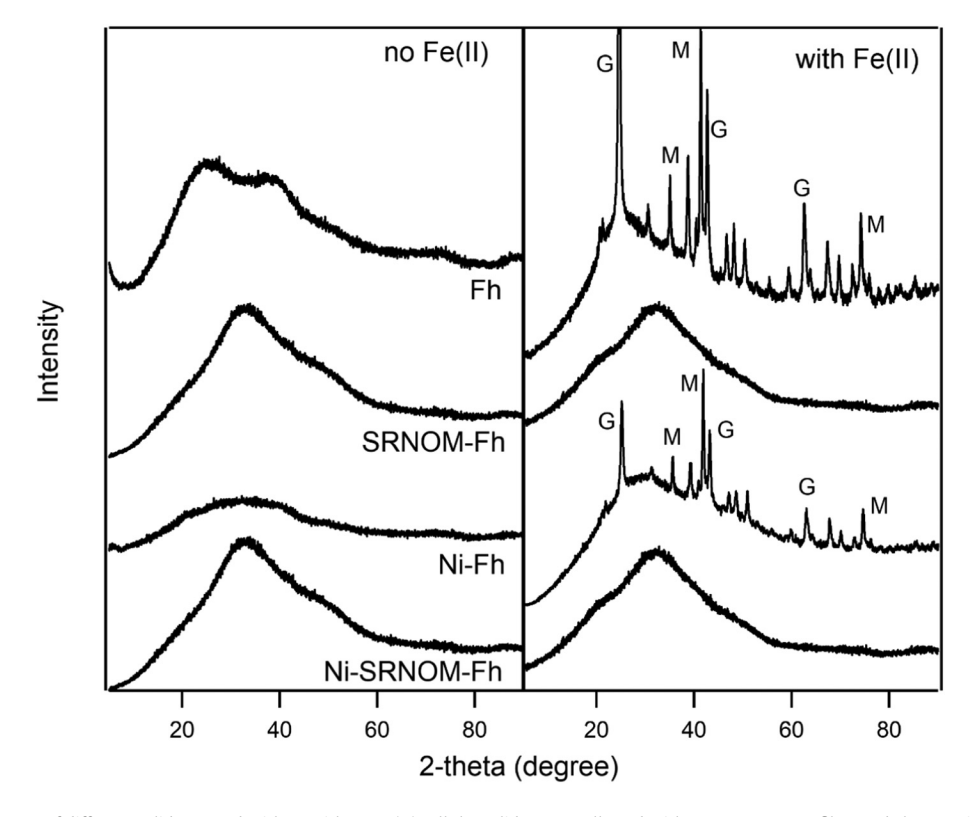


Fig. 2. X-ray diffraction pattern of different solids reacted with or without Fe(II). All the solids were collected with a 0.44 μM paper filter and characterized as wet on the filter. No background subtraction was conducted considering the less obvious diffraction of 2-line Fh. The bump around 30 degrees is related to the paper filter. Note: G = goethite, M = magnetite.

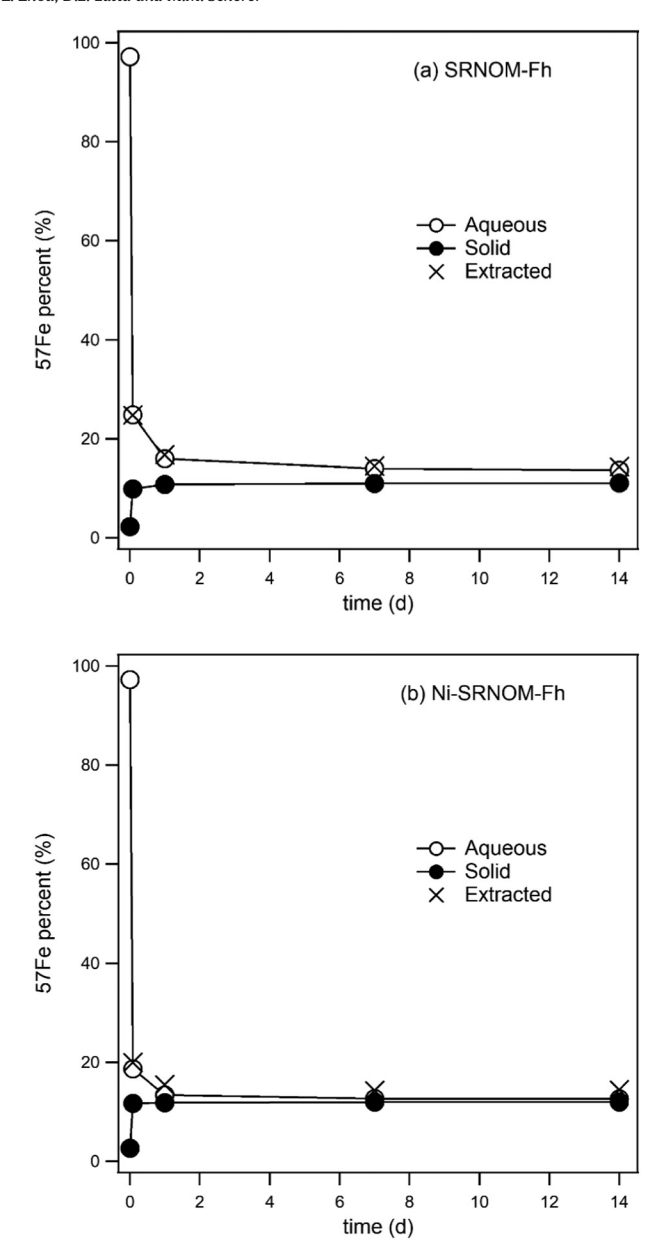


Fig. 3. The ⁵⁷Fe percent in aqueous Fe(II), extracted Fe and the residual Fe after reacting 1 mM ⁵⁷Fe(II) with (a) SRNOM-Fh in the presence of 1 mM Ni, and (b) Ni-SRNOM-Fh. Experimental condition: 10 mM PIPES buffer at pH 7.0, 10 mM Fe(III) from SRNOM-Fh or Ni-SRNOM-Fh.

there was no distinguishable Ni change in the solid phase between the experiments with and without Fe(II) (Table S4 and Fig. S2). This different effect on Ni stability between Ni-Fh and Ni-SRNOM-Fh is likely related to whether transformation to secondary minerals occurred or not in the presence of Fe(II).

To track the transformation of Ni-Fh and Ni-SRNOM-Fh, we measured the samples reacted with or without Fe(II) over fourteen days using XRD (Fig. 2). We found that reacting Ni-Fh with 1 mM Fe(II) resulted in the formation of magnetite and goethite, similar to the experiment with Fh with adsorbed Ni. This suggests neither coprecipitated nor adsorbed Ni used under our conditions changes the species of secondary Fe minerals, although the ratio of secondary Fe minerals may vary (Liu et al., 2016). In contrast to Ni-Fh, there was no measurable secondary Fe mineral formed after reacting Ni-SRNOM-Fh with Fe(II), similar to what we observed with SRNOM-Fh. Compared to Ni, the coprecipitated SRNOM has a stronger effect on the magnetic ordering of Fh (Fig. S1) and is also shown to be more inhibitive on Fh

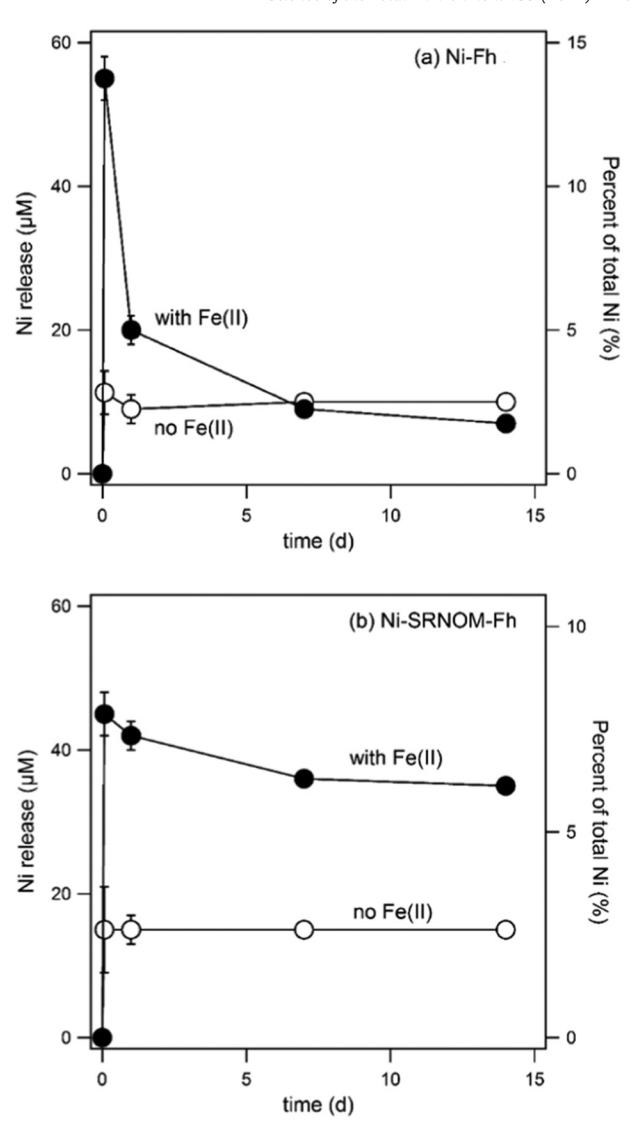


Fig. 4. The concentration of Ni that was released into the aqueous phase from (a) Ni-Fh coprecipitate and (b) Ni-SRNOM-Fh coprecipitate with or without the presence of 1 mM Fe(II) at 10 mM PIPES buffer (pH 7.0). The total Ni concentration was 460 μ M in the Ni-Fh system and 620 μ M in the Ni-SRNOM-Fh system.

transformation. Even though there was no secondary mineral formed after reacting Ni-SRNOM-Fh with Fe(II), Fe atom exchange between aqueous Fe(II) and Fe(III) may occur and change the distribution of Ni (Zhou et al., 2018; Frierdich et al., 2012).

To track the Fe atom movement between aqueous Fe(II) and Ni-SRNOM-Fh, ⁵⁷Fe was used to label aqueous Fe(II). We found 75% of Fe (II) was adsorbed by Ni-SRNOM-Fh over fourteen days, higher than the setup with SRNOM-Fh (55%, possibly due to the competition of aqueous Ni). Fe isotope mixing in the experiment with Ni-SRNOM-Fh was also faster than SRNOM-Fh, with ⁵⁷Fe percent in aqueous Fe(II) dropped from 97% to 19% in the first hour and approached the complete isotope mixing value by one day (Table S6). This faster Fe isotope mixing could be related to the higher extent of Fe(II) adsorption by Ni-SRNOM-Fh (Tables S5 and S6) (Handler et al., 2014). In addition, the mineral structure in the initial Ni-SRNOM-Fh may become more disordered than SRNOM-Fh with the incorporation of Ni (Fig. S1), thus reduce the stability of Fe(III) and contribute to a faster Fe atom exchange with aqueous Fe(II). It is interesting to note ⁵⁷Fe percentage in the extracted Fe phase is slightly higher than aqueous Fe during Fe(II) reacting with Ni-SRNOM-Fh (Fig. 4). One possible explanation is that the aqueous ⁵⁷Fe(II) initially replaced some Ni that was bound with SRNOM,

this part of Fe(II) was with a high ⁵⁷Fe percent and sluggish to further Fe atom exchange, thus increased the ⁵⁷Fe percent in the extracted Fe phase. The rapid increase in aqueous Ni concentration was consistent with this hypothesis (Fig. 4b). In general, extensive Fe atom exchanged between aqueous Fe(II) and Ni-SRNOM-Fh and caused some Ni stabilization, but the extent of Ni stabilization was less obvious than Ni-Fh where Fh was transformed by Fe(II) and Ni was extensively stabilized.

3.3. Inhibited Ni stabilization by NOM

We propose that coprecipitated SRNOM altered Fe(II)-catalyzed Fh transformation pathway, which leads to the different Ni behavior under reducing condition. For Fh and Ni-Fh, the mineral transformation was catalyzed by aqueous Fe(II), this Fe(II)-catalyzed Fh transformation was a process coupled with Fe mineral dissolution and reprecipitation, during which adsorbed Fe(II) transferred electrons to Fe(III) in Fh and caused its reductive dissolution (Eickhoff et al., 2014; Boland et al., 2014). With the dissolution of Fh, associated Ni could be released due to the loss of sorption sites (Latta et al., 2012a), and that explains the temporarily increased aqueous Ni concentration shown in Fig. 3a. After transferring electrons to structural Fe(III), the adsorbed Fe(II) was oxidized to Fe(III) and formed secondary Fe minerals (magnetite and goethite in this study). During the formation of secondary Fe minerals, the coexisted Ni, or other trace metals with similar or smaller atom radius as Fe(III), could replace structural Fe(III) in secondary Fe minerals or be incorporated into the lattice space of secondary Fe minerals (Latta et al., 2012a; Frierdich et al., 2011). The resorption of Ni during the formation of secondary Fe minerals observed in this study could be partially explained by this mechanism. In addition, the incorporated Ni should less suspect to acid extraction, and the pH 3.0 extraction conducted in this study also found less Ni extractable from Fh and Ni-Fh after reaction with Fe(II), supporting that Ni was partially incorporated into the structure of secondary Fe minerals. Except for the structural incorporation, Ni re-adsorption by secondary Fe minerals may also contribute to Ni resorption as newly formed goethite and magnetite may offer available sites for Ni absorption or surface adsorption (Vu et al., 2013; Ford et al., 1997). But note the surface area of secondary Fe minerals is much smaller compared to the nanosized Fh (Vu et al., 2013), and Ni loading in this study was relatively high, as such Ni readsorption by secondary Fe minerals may not fully account for the enhanced Ni removal in the presence of Fe(II).

With coprecipitated SRNOM, the Fe(II)-catalyzed Fh transformation pathway was altered. As shown in our previous study and others (Chen et al., 2015; Zhou et al., 2018), more Fh was preserved with the increasing of C/Fe ratio until the transformation was inhibited. Some associated trace metals were also suggested to change the rate and extent of Fh transformation (Liu et al., 2016). It is not surprising that no Fh transformation was observed in SRNOM-Fh and Ni-SRNOM-Fh coprecipitate considering the high C/Fe ratio (1.2). But it is challenging to explain the Ni release from Ni-SRNOM-Fh and the slightly increased residual Ni in SRNOM-Fh during the reaction with Fe(II), especially with limited information about Ni binding between SRNOM and Fh. Based on a recent study of Ni adsorption to OM-Fh coprecipitate (Wang et al., 2020), we estimated there was 70–80% of Ni directly bonded to Fh in SRNOM-Fh. The percent of Fh bonded Ni may be even higher in Ni-SRNOM-Fh. Ni that complexing or chelating with certain functional groups in SRNOM, such as -COOH and -OH, can be replaced by Fe(II), leading to the release of pre-associated Ni (Santschi et al., 1999). Aqueous Fe(II) can compete with Ni for the adsorption sites in SRNOM and Fh, it also experienced redox reaction with Fh as suggested in our ⁵⁷Fe tracer study. During the extensive Fe atom exchange between aqueous Fe(II) and structural Fe(III) in Ni-SRNOM-Fh or SRNOM-Fh, precoprecipitated Ni or adsorbed Ni may slightly redistribute, which can be supported by the release of pre-coprecipitated Ni and decreased extractable Ni (5%) in SRNOM-Fh. But please note the Ni stabilization in

this situation was less significant compared to Fh and Ni-Fh where secondary Fe minerals were formed.

4. Conclusion

Our results showed that coprecipitated NOM did not significantly change Ni adsorption to Fh, but in the presence of Fe(II), the coprecipitate NOM inhibited Fh transformation thus resulted in different Ni fate in Fh with or without NOM. In Fh and Ni-Fh, Ni was incorporated into secondary Fe minerals during Fe(II)-catalyzed transformation and it's overall stability (as measured by resistance to mild acid extraction) increased which may make it less available to microbes or plants. Fh transformation to secondary minerals was inhibited by NOM. However, we observed Fe isotope mixing between aqueous Fe(II) and Fe (III) in SRNOM-Fh and Ni-SRNOM-Fh. This Fe atom mixing, however, did not result in obvious Ni stabilization as we found in Fh and Ni-Fh. In general, the presence of NOM limited Ni incorporating into secondary Fe minerals that with higher crystallinity and stability, and may make Fh associated Ni less stable and more susceptible to pH variations in sediments or soils.

CRediT authorship contribution statement

Zhe Zhou: Conceptualization, Investigation, Writing.Drew E. Latta: Conceptualization, Supervision.Michelle M. Scherer: Conceptualization, Writing, Supervision, Funding acquisition.

Declaration of competing interest

The authors declare that they have no known competing financial interests or personal relationships that could have appeared to influence the work reported in this paper.

Acknowledgements

The authors thank the China Scholarship Council (CSC) for the financial support to Zhe Zhou. Additional support for this work was provided by the National Science Foundation (NSF) through the NSF Division of Chemistry under Grant No. 1708467.

Appendix A. Supplementary data

Supplementary data to this article can be found online at https://doi.org/10.1016/j.scitotenv.2020.142612.

References

Boland, D.D., Collins, R.N., Miller, C.J., Glover, C.J., Waite, T.D., 2014. Effect of solution and solid-phase conditions on the Fe(II)-accelerated transformation of ferrihydrite to lepidocrocite and goethite. Environ. Sci. Technol. 48 (10), 5477–5485.

Bolanz, R.M., Wierzbicka-Wieczorek, M., ČaploviČová, M.r., Uhlík, P., Göttlicher, J.r., Steininger, R., Majzlan, J., 2013. Structural incorporation of As5+ into hematite. Environ. Sci. Technol. 47 (16), 9140–9147.

Bruemmer, G., Gerth, J., Tiller, K., 1988. Reaction kinetics of the adsorption and desorption of nickel, zinc and cadmium by goethite. I. Adsorption and diffusion of metals. J. Soil Sci. 39 (1), 37–52.

Chanda, P., Zhou, Z., Latta, D.E., Scherer, M.M., Beard, B.L., Johnson, C.M., 2020. Effect of organic C on stable Fe isotope fractionation and isotope exchange kinetics between aqueous Fe(II) and ferrihydrite at neutral pH. Chem. Geol. 531, 119344.

Chen, C.M., Kukkadapu, R., Sparks, D.L., 2015. Influence of coprecipitated organic matter on Fe-(aq)(2+)-catalyzed transformation of Ferrihydrite: implications for carbon dynamics. Environ. Sci. Technol. 49 (18), 10927–10936.

Cornell, R.M., Schwertmann, U., 2003. The Iron Oxides: Structure, Properties, Reactions, Occurrences and Uses. John Wiley & Sons.

Coughlin, B.R., Stone, A.T., 1995. Nonreversible adsorption of divalent metal-ions (Mn-li, Co-li Ni-li Cu-li and Pb-li) onto goethite - effects of acidification, Fe-li addition, and picolinic-acid addition. Environ. Sci. Technol. 29 (9), 2445–2455.

Eickhoff, M., Obst, M., Schröder, C., Hitchcock, A.P., Tyliszczak, T., Martinez, R.E., Robbins, L.J., Konhauser, K.O., Kappler, A., 2014. Nickel partitioning in biogenic and abiogenic ferrihydrite: the influence of silica and implications for ancient environments. Geochim. Cosmochim. Acta 140, 65–79.

- Fei, Y., Hua, J., Liu, C., Li, F., Zhu, Z., Xiao, T., Chen, M., Gao, T., Wei, Z., Hao, L., 2018. Aqueous Fe (II)-induced phase transformation of ferrihydrite coupled adsorption/immobilization of rare earth elements. Minerals 8 (8), 357.
- Ford, R.G., Bertsch, P.M., Farley, K.J., 1997. Changes in transition and heavy metal partitioning during hydrous iron oxide aging. Environ. Sci. Technol. 31 (7), 2028–2033.
- Frierdich, A.J., Catalano, J.G., 2012. Controls on Fe (II)-activated trace element release from goethite and hematite. Environ. Sci. Technol. 46 (3), 1519–1526.
- Frierdich, A.J., Luo, Y., Catalano, J.G., 2011. Trace element cycling through iron oxide minerals during redox-driven dynamic recrystallization. Geology 39 (11), 1083–1086.
- Frierdich, A.J., Scherer, M.M., Bachman, J.E., Engelhard, M.H., Rapponotti, B.W., Catalano, J.G., 2012. Inhibition of trace element release during Fe (II)-activated recrystallization of Al-, Cr-, and Sn-substituted goethite and hematite. Environ. Sci. Technol. 46 (18), 10031–10039.
- Gorski, C.A., Fantle, M.S., 2017. Stable mineral recrystallization in low temperature aqueous systems: a critical review. Geochim. Cosmochim. Acta 198, 439–465.
- Gorski, C.A., Scherer, M.M., 2011. Fe2+ sorption at the Fe oxide-water interface: a revised conceptual framework. Aquatic Redox Chemistry 1071, 477–517.
- Handler, R.M., Frierdich, A.J., Johnson, C.M., Rosso, K.M., Beard, B.L., Wang, C.M., Latta, D.E., Neumann, A., Pasakarnis, T., Premaratne, W., Scherer, M.M., 2014. Fe(II)-catalyzed recrystallization of goethite revisited. Environ. Sci. Technol. 48 (19), 11302–11311.
- Hansel, C.M., Benner, S.G., Neiss, J., Dohnalkova, A., Kukkadapu, R.K., Fendorf, S., 2003. Secondary mineralization pathways induced by dissimilatory iron reduction of ferrihydrite under advective flow. Geochim. Cosmochim. Acta 67 (16), 2977–2992.
- Hansel, C.M., Benner, S.G., Fendorf, S., 2005. Competing Fe (II)-induced mineralization pathways of ferrihydrite. Environmental Science & Technology 39 (18), 7147–7153.
- Jang, J.-H., Dempsey, B.A., Catchen, G.L., Burgos, W.D., 2003. Effects of Zn (II), Cu (II), Mn (II), Fe (II), NO3-, or SO42- at pH 6.5 and 8.5 on transformations of hydrous ferric oxide (HFO) as evidenced by Mössbauer spectroscopy. Colloids Surf. A Physicochem. Eng. Asp. 221 (1-3), 55-68.
- Joshi, P., Fantle, M.S., Larese-Casanova, P., Gorski, C.A., 2017. Susceptibility of goethite to Fe2+-catalyzed recrystallization over time. Environ. Sci. Technol. 51 (20), 11681–11691.
- Kaiser, K., Guggenberger, G., 2000. The role of DOM sorption to mineral surfaces in the preservation of organic matter in soils. Org. Geochem. 31 (7), 711–725.
- Kappler, A., Benz, M., Schink, B., Brune, A., 2004. Electron shuttling via humic acids in microbial iron (III) reduction in a freshwater sediment. FEMS Microbiol. Ecol. 47 (1), 85–92.
- Lalonde, K., Mucci, A., Ouellet, A., Gelinas, Y., 2012. Preservation of organic matter in sediments promoted by iron. Nature 483 (7388), 198–200.
- Latta, D.E., Gorski, C.A., Scherer, M.M., 2012a. Influence of Fe2+-catalysed iron oxide recrystallization on metal cycling. Biochem. Soc. Trans. 40, 1191–1197.
- Latta, D.E., Bachman, J.E., Scherer, M.M., 2012b. Fe electron transfer and atom exchange in goethite: influence of Al-substitution and anion sorption. Environ. Sci. Technol. 46 (19), 10614–10623.
- Li, Y., Yu, S., Strong, J., Wang, H., 2012. Are the biogeochemical cycles of carbon, nitrogen, sulfur, and phosphorus driven by the "Fe III-Fe II redox wheel" in dynamic redox environments? J. Soils Sediments 12 (5), 683–693.
- Liu, C., Zhu, Z., Li, F., Liu, T., Liao, C., Lee, J.-J., Shih, K., Tao, L., Wu, Y., 2016. Fe (II)-induced phase transformation of ferrihydrite: the inhibition effects and stabilization of divalent metal cations. Chem. Geol. 444, 110–119.
- Marshall, T.A., Morris, K., Law, G.T., Livens, F.R., Mosselmans, J.F.W., Bots, P., Shaw, S., 2014. Incorporation of uranium into hematite during crystallization from ferrihydrite. Environ. Sci. Technol. 48 (7), 3724–3731.
- Martinez, C.E., McBride, M.B., 1998. Coprecipitates of Cd, Cu, Pb and Zn in iron oxides: solid phase transformation and metal solubility after aging and thermal treatment. Clay Clay Miner. 46 (5), 537–545.

- Melton, E.D., Swanner, E.D., Behrens, S., Schmidt, C., Kappler, A., 2014. The interplay of microbially mediated and abiotic reactions in the biogeochemical Fe cycle. Nat. Rev. Microbiol. 12, 797.
- Mitsunobu, S., Muramatsu, C., Watanabe, K., Sakata, M., 2013. Behavior of antimony (V) during the transformation of ferrihydrite and its environmental implications. Environ. Sci. Technol. 47 (17), 9660–9667.
- Muramatsu, C., Sakata, M., Mitsunobu, S., 2012. Immobilization of arsenic (V) during the transformation of ferrihydrite: a direct speciation study using synchrotron-based XAFS spectroscopy. Chem. Lett. 41 (3), 270–271.
- Pedersen, H.D., Postma, D., Jakobsen, R., Larsen, O., 2005. Fast transformation of iron oxyhydroxides by the catalytic action of aqueous Fe (II). Geochim. Cosmochim. Acta 69 (16), 3967–3977.
- Santschi, P.H., Guo, L., Means, J.C., Ravichandran, M., 1999. Natural organic matter binding of trace metals and trace organic contaminants in estuaries. Biogeochemistry of Gulf of Mexico Estuaries 347–380.
- Scheinost, A.C., Abend, S., Pandya, K.I., Sparks, D.L., 2001. Kinetic controls on Cu and Pb sorption by ferrihydrite. Environ. Sci. Technol. 35 (6), 1090–1096.
- Schwertmann, U., 1966. Inhibitory effect of soil organic matter on the crystallization of amorphous ferric hydroxide. Nature 212 (5062), 645.
- Schwertmann, U., Cornell, R.M., 2008. Iron Oxides in the Laboratory: Preparation and Characterization. John Wiley & Sons.
- Schwertmann, U.t., Fischer, W., 1973. Natural "amorphous" ferric hydroxide. Geoderma 10 (3), 237–247.
- Shimizu, M., Zhou, J., Schröder, C., Obst, M., Kappler, A., Borch, T., 2013. Dissimilatory reduction and transformation of ferrihydrite-humic acid coprecipitates. Environ. Sci. Technol. 47 (23), 13375–13384.
- Society, I. H. S. Elemental Compositions and Stable Isotopic Ratios of IHSS Samples. (accessed May 16, 2018).
- ThomasArrigo, L.K., Kaegi, R., Kretzschmar, R., 2019. Ferrihydrite growth and transformation in the presence of ferrous Iron and model organic ligands. Environ. Sci. Technol. 53 (23), 13636–13647.
- Tronc, E., Belleville, P., Jolivet, J.P., Livage, J., 1992. Transformation of ferric hydroxide into spinel by Fe(II) adsorption. Langmuir 8 (1), 313–319.
- Van Cappellen, P., Wang, Y., 1996. Cycling of iron and manganese in surface sediments; a general theory for the coupled transport and reaction of carbon, oxygen, nitrogen, sulfur, iron, and manganese. Am. J. Sci. 296 (3), 197–243.
- Voelker, B.M., Morel, F.M., Sulzberger, B., 1997. Iron redox cycling in surface waters: effects of humic substances and light. Environ. Sci. Technol. 31 (4), 1004–1011.
- von Lutzow, M., Kogel-Knabner, I., Ekschmitt, K., Matzner, E., Guggenberger, G., Marschner, B., Flessa, H., 2006. Stabilization of organic matter in temperate soils: mechanisms and their relevance under different soil conditions - a review. Eur. J. Soil Sci. 57 (4), 426-445.
- Vu, H.P., Shaw, S., Brinza, L., Benning, L.G., 2013. Partitioning of Pb (II) during goethite and hematite crystallization: implications for Pb transport in natural systems. Appl. Geochem. 39, 119–128.
- Wang, P., Lu, Y., Hu, S., Tian, L., Liang, Y., Shi, Z., 2020. Kinetics of Ni reaction with organic matter-ferrihydrite composites: experiments and modeling. Chem. Eng. J. 379, 122306.
- Weber, K.A., Achenbach, L.A., Coates, J.D., 2006. Microorganisms pumping iron: anaerobic microbial iron oxidation and reduction. Nat. Rev. Microbiol. 4 (10), 752.
- Zhou, Z., Latta, D.E., Noor, N., Thompson, A., Borch, T., Scherer, M.M., 2018. Fe (II)-catalyzed transformation of organic matter–ferrihydrite coprecipitates: a closer look using Fe isotopes. Environ. Sci. Technol. 52 (19), 11142–11150.